

Effects of excess Fe on upper critical field and magnetotransport in $\text{Fe}_{1+y}(\text{Te}_{1-x}\text{S}_x)_z$ Hechang Lei (雷和畅),¹ Rongwei Hu (胡荣伟),^{1,*} E. S. Choi,² J. B. Warren,³ and C. Petrovic¹¹*Condensed Matter Physics and Materials Science Department, Brookhaven National Laboratory, Upton, New York 11973, USA*²*NHMFL/Physics, Florida State University, Tallahassee, Florida 32310, USA*³*Instrumentation Division, Brookhaven National Laboratory, Upton, New York 11973, USA*

(Received 10 March 2010; revised manuscript received 23 April 2010; published 20 May 2010)

We have investigated the upper critical field anisotropy and magnetotransport properties of $\text{Fe}_{1.14(1)}\text{Te}_{0.91(2)}\text{S}_{0.09(2)}$ single crystals in stable magnetic fields up to 35 T. The results show that $\mu_0 H_{c2}(T)$ along the c axis and in the ab plane exhibit saturation at low temperatures. The anisotropy of $\mu_0 H_{c2}(T)$ decreases with decreasing temperature, becoming nearly isotropic for $T \rightarrow 0$. Our analysis indicates that the spin-paramagnetic pair breaking with spin-orbital scattering is responsible for the behavior of $\mu_0 H_{c2}(T)$. Furthermore, from analysis of the normal-state properties, we show evidence that the excess Fe is a key factor determining the normal- and superconducting-state physical properties.

DOI: [10.1103/PhysRevB.81.184522](https://doi.org/10.1103/PhysRevB.81.184522)

PACS number(s): 74.62.Bf, 74.10.+v, 74.20.Mn, 74.70.Dd

I. INTRODUCTION

Iron-based superconductors have generated a great deal of interests due to exotic physical and chemical properties such as high transition temperature T_c (above 50 K) in layered structure without copper oxygen planes, spin-fluctuation spectrum dominated by two-dimensional (2D) incommensurate excitations comparable to high- T_c cuprates and multi-orbital physics with active spin, charge, and orbital degrees of freedom.¹⁻⁷ Simple binary FeSe_x , $\text{Fe}(\text{Te}_{1-x}\text{Se}_x)_z$, and $\text{Fe}_{1+y}(\text{Te}_{1-x}\text{S}_x)_z$ (Refs. 8–10) share common characteristics with other iron-based superconductors: a square-planar lattice of Fe with tetrahedral coordination and similar Fermi-surface topology.¹¹ On the other hand, they exhibit some distinctive features such as the absence of charge reservoir, significant pressure effect,¹² and strongly magnetic excess Fe in Fe(2) site providing local moments that are expected to persist even if the antiferromagnetic order is suppressed by doping or pressure.¹³ Furthermore, superconductivity in $\text{Fe}_{1+y}(\text{Te}_{1-x}\text{S}_x)_z$ develops from nonmetallic conductivity which is different from metallic resistivity above T_c in all other iron-based superconductors.^{10,14}

There are two remarkable common characteristics in $\mu_0 H_{c2}$ - T phase diagram of iron-based superconductors. In ternary and quaternary iron-pnictide superconductors (122 and 1111 systems), $\mu_0 H_{c2,c}(T)$ shows pronounced upturn or positive temperature curvature far below T_c without saturation. In contrast, $\mu_0 H_{c2,ab}(T)$ exhibits a downturn curvature with decreasing temperature.^{15,16} The former can be explained by two-band theory with high (1111) or low (122 systems) intraband diffusivity ratio of electron band to hole band and the latter is commonly ascribed to the spin-paramagnetic effect.¹⁶⁻²⁰

Here we report comprehensive study of the upper critical-field anisotropy and magnetotransport properties of $\text{Fe}_{1.14(1)}(\text{Te}_{0.91(2)}\text{S}_{0.09(2)})_z$ single crystals in stable magnetic fields up to 35 T. We observe that enhanced spin-paramagnetic effect is dominant in both $\mu_0 H_{c2,c}(T)$ and $\mu_0 H_{c2,ab}(T)$. We conclude that the root cause of that enhancement and the anomalous normal-state electronic-transport properties is the existence of excess Fe(2) iron. As opposed

to 122 and 1111 iron-pnictide superconductors derived from stoichiometric $\text{Ba}(\text{Sr})\text{Fe}_2\text{As}_2$ and LaOFeAs parent compounds, the width of material formation and subtle iron stoichiometry is rather important in superconductors derived from Fe_{1+y}Te .

II. EXPERIMENT

Single crystals of $\text{Fe}(\text{Te},\text{S})$ were grown by self-flux method and their crystal structure was analyzed in the previous report.¹⁴ The elemental and microstructure analysis on particular crystal used in this study showed $\text{Fe}_{1.14(1)}(\text{Te}_{0.91(2)}\text{S}_{0.09(2)})_z$ stoichiometry and will be denoted as S-09 in the following for brevity. Electrical-transport measurements were performed using a four-probe configuration with current flowing in the ab plane of tetragonal structure in dc magnetic fields up to 9 T in a Quantum Design Physical Property Measurement System (PPMS-9) from 1.8 to 200 K and up to 35 T in an Oxford Heliox cryostat with resistive magnet down to 0.3 K at the National High Magnetic Field Laboratory (NHMFL) in Tallahassee, FL.

III. RESULTS AND DISCUSSIONS

Figures 1(a) and 1(b) show the temperature-dependent ab -plane electrical resistivity $\rho_{ab}(T)$ of S-09 below 15 K in magnetic fields from 0 to 9 T for $H \parallel ab$ and $H \parallel c$. With increasing magnetic fields, the resistivity transition widths are slightly broader. The onset of superconductivity shifts to lower temperatures gradually for both magnetic field directions but the trend is more obvious for $H \parallel c$ than $H \parallel ab$. The shape and broadening of $\rho_{ab}(T)$ for $H \parallel c$ is comparable to 122 system²¹ but quite different from 1111 system¹⁸ where it was explained by the vortex-liquid state similar to cuprates.²²⁻²⁴ Hence, it can be concluded that the vortex-liquid state region is narrower or even absent in S-09. This is similar to $\text{Fe}_{1+y}(\text{Te}_{1-x}\text{Se}_x)_z$.²⁵

The upper critical field $\mu_0 H_{c2}(T)$ corresponding to temperatures where the resistivity drops to 90%, 50%, and 10% of the normal-state resistivity $\rho_{n,ab}(T, H)(T_{c, \text{onset}})$ is shown in Fig. 1(c). The normal-state resistivity $\rho_{n,ab}(H, T)$ was deter-

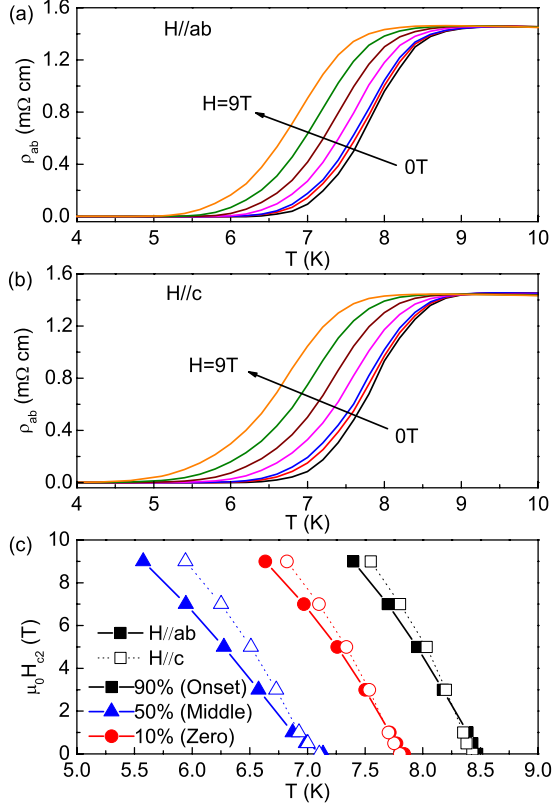


FIG. 1. (Color online) (a) and (b) Temperature dependence of $\rho_{ab}(T)$ of S-09 at fixed fields (0, 0.5, 1, 3, 5, 7, and 9 T) for $H//ab$ plane and $H//c$ axis below 15 K, respectively. (c) Temperature dependence of the resistive upper critical field $\mu_0 H_{c2}(T)$ corresponding three defined temperatures at low fields.

mined by linearly extrapolating the normal-state behavior above the onset of superconductivity in $\rho_{ab}(T)$ curves [same as for $\rho_{ab}(H)$ curves]. The slope of $\mu_0 H_{c2}(T_c)$ obtained from linear fitting the curves of $\mu_0 H_{c2}(T)$ near T_c for all defined temperatures are listed in Table I. The values of orbital pair-breaking field $\mu_0 H_{c2}^*(0)$ corresponding to the conventional one-band Werthamer-Helfand-Hohenberg (WHH) theory²⁶ $\mu_0 H_{c2}^*(0) = -0.693(d\mu_0 H_{c2}/dT)_{T_c} T_c$ are also listed in Table I.

Superconductivity is suppressed by increasing magnetic field up to 35 T and the transition of $\rho_{ab}(H)$ curves are shifted to lower magnetic fields at higher measuring temperature [Figs. 2(a) and 2(b)]. At 0.3 K, the lowest temperature of our measurement we observe no superconductivity up to 35 T for both crystallographic directions, indicating that the upper critical field $\mu_0 H_{c2}(0)$ of $Fe_{1+y}(Te_{1-x}S_x)_z$ with same doping level is lower than that of $Fe_{1+y}(Te_{1-x}Se_x)_z$.²⁵ Figure

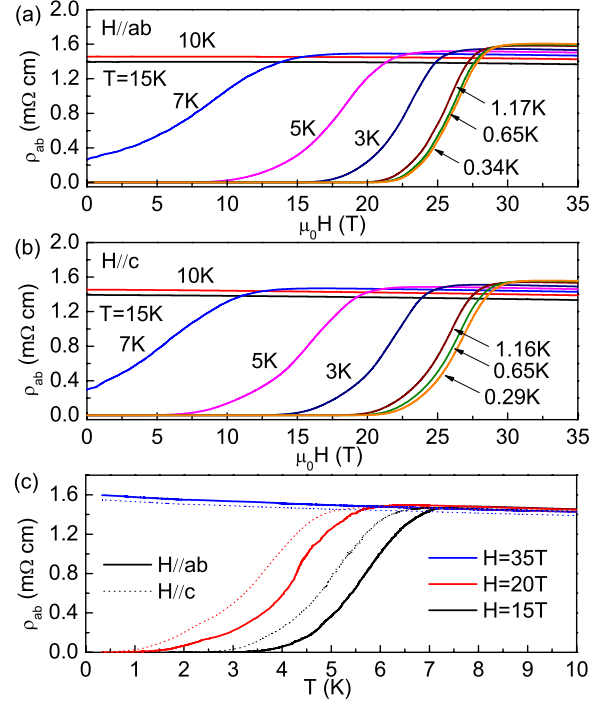


FIG. 2. (Color online) Field dependence of $\rho_{ab}(H)$ measured at various temperatures in dc magnetic fields up to 35 T for (a) $H//ab$ and (b) $H//c$. (c) Temperature dependence of $\rho_{ab}(T)$ at high magnetic fields from 15 to 35 T (15, 20, and 35 T).

2(c) shows the temperature dependence of resistivity at high magnetic fields. The superconductivity above 0.3 K is suppressed when $\mu_0 H=35$ T, irrespective of the direction of field, consistent with the results of $\rho_{ab}(H)$ measurement. The superconducting transition widths are only slightly broader even at 20 T, indicating that the vortex-liquid state in S-09 is narrow not only in low-field high temperature but also in high-field low-temperature region.

From the results of $\rho_{ab}(H)$ and $\rho_{ab}(T)$ at low and high field, we construct the $\mu_0 H_{c2}(T)-T$ phase diagram [Figs. 3(a) and 3(b)]. There is a linear increase in $\mu_0 H_{c2}(T)$ with decreasing temperature near T_c and a saturation trend away from T_c irrespective of field direction, similar to $Fe_{1+y}(Te_{1-x}Se_x)_z$.²⁵ This is different from 1111 and 122 system, which exhibit upturn or linear behavior at low temperature for $\mu_0 H_{c2}(T)$ ascribed to two-band effect.^{15,16} The $\mu_0 H_{c2,onset}(0)$ is about 28 T for both field directions. This is much smaller than the values predicted by WHH formalism with only considering orbital pair-breaking effect [Table I, Fig. 3(c) black lines].

TABLE I. $(d\mu_0 H_{c2}/dT)_{T_c}$ and derived $\mu_0 H_{c2}^*(0)$ data at three defined temperatures using WHH formula. $\mu_0 H_{c2,ab}^*(0)$ and $\mu_0 H_{c2,c}^*(0)$ are the ab -plane and c -axis orbital-limited upper critical fields at $T=0$ K.

$Fe_{1.14(1)}Te_{0.91(2)}S_{0.09(2)}$	T_c (K)	$(d\mu_0 H_{c2}/dT)_{T_c}, H//ab$ (T/K)	$(d\mu_0 H_{c2}/dT)_{T_c}, H//c$ (T/K)	$\mu_0 H_{c2,ab}^*(0)$ (T)	$\mu_0 H_{c2,c}^*(0)$ (T)
Onset	8.47	12.82	8.44	75.25	49.54
Middle	7.84	10.18	8.21	55.31	44.61
Zero	7.14	8.58	6.10	42.45	30.18

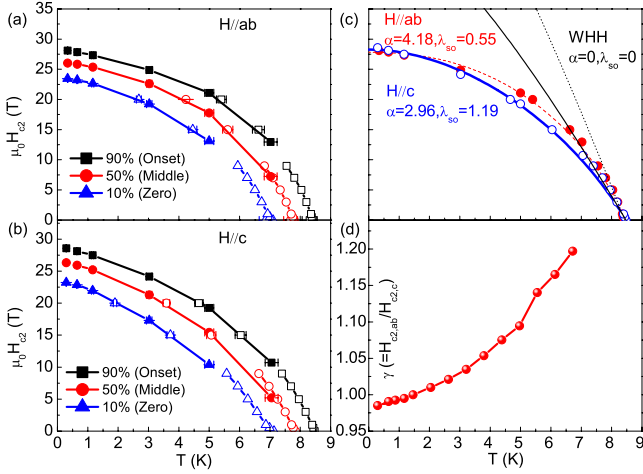


FIG. 3. (Color online) Temperature dependence of the resistive upper critical field $\mu_0 H_{c2}(T)$ of S-09 for (a) $H\parallel ab$ and (b) $H\parallel c$ derived from $\rho_{ab}(T)$ (open symbols) and $\rho_{ab}(H)$ (closed symbols) curves. (c) Analysis of $\mu_0 H_{c2,onset}(T)$ for $H\parallel ab$ (closed circles) and $H\parallel c$ (open circles) using the WHH theory without (dotted line for $H\parallel ab$ and thin solid line for $H\parallel c$) and with (dashed line for $H\parallel ab$ and thick solid line for $H\parallel c$) spin-paramagnetic effect and spin-orbital scattering. (d) The anisotropy of the upper critical field, $\gamma = H_{c2,ab}(T)/H_{c2,c}(T)$, as a function of temperature.

In what follows we consider the contribution of spin-paramagnetic effect and its origin. Only the $\mu_0 H_{c2,onset}(T)$ were chosen for further analysis.^{16,27} The effects of Pauli-spin paramagnetism and spin-orbit scattering were included in the WHH theory through the Maki parameters α and λ_{so} .^{26,28} We found it necessary to introduce $\lambda_{so} \neq 0$ in $\mu_0 H_{c2}(T)$ fits, unlike for $\text{Fe}_{1+y}(\text{Te}_{1-x}\text{Se}_x)_z$.^{25,27} The results [Fig. 3(c)] indicate that the spin-paramagnetic effect is the dominant pair-breaking mechanism in S-09 for both $H\parallel ab$ and $H\parallel c$. The calculated zero-temperature Pauli-limited field²⁸ $H_p(0) = \sqrt{2}H_{c2}^*(0)/\alpha$ using α obtained from $\mu_0 H_{c2}(T)$ fits and zero-temperature coherence length $\xi(0)$ estimated with Ginzburg-Landau formula $\mu_0 H_{c2}(0) = \Phi_0/2\pi\xi(0)$ (where $\Phi_0 = 2.07 \times 10^{-15}$ Wb) are listed in Table II. The $\mu_0 H_p(0)$ is smaller than $\mu_0 H_{c2}(0)$ due to the large value of α . Since $\text{Fe}_{1+y}\text{Te}_{1-x}\text{S}_x$ superconductors are in the dirty limit,²⁹ the Fulde-Ferrell-Larkin-Ovchinnikov state at high fields is unlikely because short mean-free path will remove any momentum anisotropy.^{30,31} The two-band theory,³² which is applicable to the 1111 system, did not yield satisfactory fits (not shown here).

Temperature dependence of anisotropy of $\mu_0 H_{c2}(T)$, $\gamma = H_{c2,ab}(T)/H_{c2,c}(T)$, is shown in Fig. 3(d) as a function of

temperature T . The value of γ for S-09 is smaller than that of $\text{Fe}_{1+y}(\text{Te}_{1-x}\text{Se}_x)_z$ at high temperature^{25,33} and it decreases gradually to 1 with decreasing temperature. Values of γ decrease to 1 below $T=1$ K, which has also been observed in $\text{Fe}_{1+y}(\text{Te}_{0.6}\text{Se}_{0.4})_z$.^{25,33}

Why are there large Maki parameter α and nonzero λ_{so} ? First, the Maki parameter can be enhanced due to disorder.^{27,34} In this system, disorder can be induced by Te(S) substitution/vacancies and excess Fe in Fe(2) site, resulting in the enhancement of spin-paramagnetic effect. Second, according to the expression of $\mu_0 H_p(0)$ with strong-coupling correction considering electron-boson and electron-electron interaction:^{27,35,36} $\mu_0 H_p(0) = 1.86(1+\lambda)^\varepsilon \eta_\Delta \eta_{ib}(1-I)$, where η_Δ describes the strong-coupling intraband correction for the gap, I is the Stoner factor $I = N(E_F)J$, $N(E_F)$ is the electronic density of states per spin at the Fermi energy level E_F , J is an effective exchange integral, η_{ib} is introduced to describe phenomenologically the effect of the gap anisotropy, λ is electron-boson coupling constant, and $\varepsilon=0.5$ or 1. Since the $N(E_F)$ of FeS is larger than that of FeSe,¹¹ it is likely that the $N(E_F)$ of $\text{Fe}_{1+y}(\text{Te}_{1-x}\text{S}_x)_z$ is larger than that of $\text{Fe}_{1+y}(\text{Te}_{1-x}\text{Se}_x)_z$ with same doping content, which will lead to the larger α . It is consistent with the previous reported result.²⁵ Third, $\mu_0 H_p(0)$ can be decreased, i.e., larger α , if the Stoner factor increases via enhancement of J by Ruderman-Kittel-Kasuya-Yosida interaction between local magnetic moments of Fe(2) with itinerant electrons. We expect low content of S doping to have small effect on high $N(E_F)$.^{11,13} On the other hand, large λ_{so} can also be explained via increasing Kondo-type scattering from excess Fe, consistent with the definition of λ_{so} , which is proportional to the spin-flip scattering rate.^{26,28}

In the next section, we study the normal-state properties systematically. Figure 4(a) shows the temperature dependence of $\rho_{ab}(T)$ in zero field from 1.8 to 300 K. As seen from the data, S-09 exhibits a nonmetallic resistivity behavior in normal state, in agreement with measurements on polycrystals.¹⁰ Similar behavior has also been observed in FeTe with low Se-content doping,^{9,37,38} ascribed to 2D weak localization.³⁸ However, our analysis indicates that $\rho_{ab}(T)$ can originate from Kondo-type scattering. It can be seen that the normal-state resistivity at zero field satisfies Hamann's equation perfectly [Fig. 4(a)]: $\rho = \rho_{imp} + \rho_0 [1 - \ln(T/T_K)] / \{(\ln^2(T/T_K) + \pi^2 S(S+1))^{1/2}\}$, where ρ_{imp} is an temperature-independent impurity scattering resistivity, ρ_0 is proportional to the concentration of the local magnetic moment, T_K is Kondo temperature, and S is set as 1/2.³⁹ The fitted parameters are $\rho_{imp} = 0.76(1)$ m Ω cm, $\rho_0 = 0.54(1)$ m Ω cm, and $T_K = 24.3(4)$ K. Inset of Fig. 4(a) shows the region at low temperature, where it can be seen

TABLE II. Superconducting parameters of S-09 obtained from the analysis of $\mu_0 H_{c2,onset}(T)$. $\mu_0 H_{c2}^*(0)$, $\mu_0 H_p(0)$, and $\mu_0 H_{c2}(0)$ are the zero-temperature orbital-limited, Pauli-limited, and fitted upper critical fields, respectively. α and λ_{so} are the fitted Maki parameter and spin-orbital scattering constant, respectively. $\xi_{ab}(0)$ and $\xi_c(0)$ are the c -axis and ab -plane zero-temperature coherence length calculated using $\mu_0 H_{c2}(0)$, respectively.

$\mu_0 H_{c2,ab}^*(0)$ (T)	$\mu_0 H_{c2,c}^*(0)$ (T)	$\mu_0 H_{p,ab}(0)$ (T)	$\mu_0 H_{p,c}(0)$ (T)	$\mu_0 H_{c2,ab}(0)$ (T)	$\mu_0 H_{c2,c}(0)$ (T)	$\alpha_{H\parallel ab}$	$\alpha_{H\parallel c}$	$\lambda_{so,H\parallel ab}$	$\lambda_{so,H\parallel c}$	$\xi_{ab}(0)$ (nm)	$\xi_c(0)$ (nm)
75.25	49.54	25.46	23.67	27.83	28.28	4.18	2.96	0.55	1.19	3.41	3.42

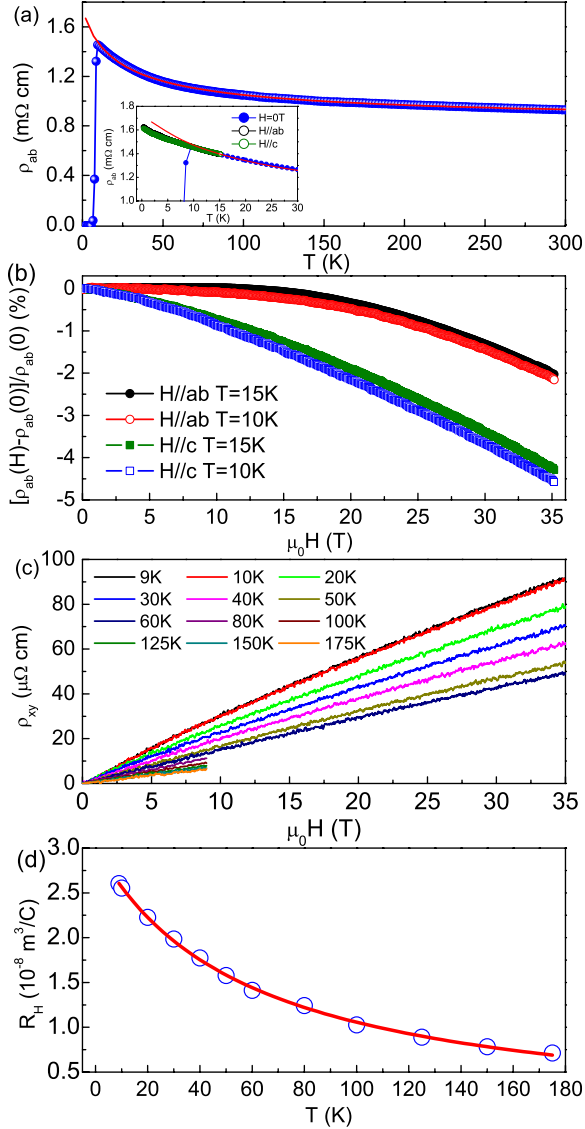


FIG. 4. (Color online) (a) Temperature dependence of $\rho_{ab}(T)$ at zero field from 1.8 to 300 K and fitted curve using Hamann's equation. Inset of (a) shows the $\rho_{ab}(T)$ at 0 and 35 T for $H//ab$ and $H//c$ (deducting the MR effects) at low temperature. (b) Field dependence of MR at different temperatures up to 35 T at 10 and 15 K. (c) Hall resistivity ρ_{xy} vs magnetic field at various temperatures, and the data above 60 K are obtained in PPMS system up to 9 T. (d) Temperature dependence of Hall coefficient R_H determined from linear fitting $\rho_{xy}(H)$ data and fitting curve using the formula described in the text.

that Hamann's equation is valid approximately down to temperatures $T \sim T_K$. It should be noted that after deducting the magnetoresistance, the normal-state resistivity at $\mu_0 H = 35$ T still increases with decreasing temperature for both field directions, showing saturation trend as expected for $\rho(T)$ of diluted impurities below T_K .⁴⁰ This behavior is an important distinction from the metallic resistivity above T_C in 1111 and 122 systems, even FeSe_x (Refs. 8, 15, and 16) because these systems do not contain excess Fe with local moment. We note that $\Delta\rho \propto \ln T$ was observed in α particle irradiated Nd(O,F)FeAs single crystals due to Kondo-type

scattering on the magnetic moments of irradiation defects.⁴¹ This effect could also contribute to $\rho \propto \ln T$ dependence in S-09 due to possible defects on Te(S) site.¹⁴

On the other hand, negative magnetoresistance (NMR) in the normal state [Fig. 4(b)] further suggests the effect of excess Fe. NMR observed in S-09 is rather unusual when compared to other iron-based superconductors, such as 1111 and 122 systems where positive MR violates Kohler scaling due to multiband effects or the depletion of density of states at the Fermi surface with temperature change.⁴² Observed NMR is most likely ascribed to suppressing incoherent Kondo spin-flip scattering, which has been intensively studied in dilute alloy systems.⁴³ The absolute values of MR increase with increasing field at the constant temperature and the MR effect is weaker with the temperature increase. Moreover, the MR effect is more pronounced for $H//ab$ than for $H//c$. Similar NMR have been seen in excess iron-doped TaSe_2 and ascribed to Kondo-type scattering.⁴⁴

Figures 4(b) and 4(c) show the magnetic field dependence of Hall resistivity ρ_{xy} and R_H determined from the slope of Hall resistivity $\rho_{xy}(H)$ at different temperatures. The positive R_H above T_C indicates that the electronic transport is dominated by hole-type carriers. We observe no abrupt change in carrier density at the temperature of magnetic transition.¹⁴ This is consistent with angle resolved photoemission spectroscopy (ARPES) and optical spectroscopy observations, implying that there is no gap at the Fermi surface below the magnetic transition. There is strong temperature dependence of R_H that increases continuously with increasing temperature. The R_H bending at low temperatures can be ascribed to skew scattering.⁴⁵ The combined influence of ordinary Hall effect R_0 and skew scattering due to Kondo-type scattering is expected to follow $R_H(T) = R_0 + A/(T - \Theta)$ dependence where Θ characterizes the strength of exchange interaction between local moments. We obtained excellent fitting results [solid line in Fig. 4(d)]. The value of Θ is $-57.9(1)$ K, which indicates that the exchange interaction between Fe is antiferromagnetic. The similar behavior has also been observed in other iron-based systems was explained by localization behavior induced by disorder, multiband effects or partial gapping Fermi surface with decreasing temperature.^{38,46,47} Furthermore, using the obtained $R_H(T=0) = 3.02 \times 10^{-8}$ m 3 /C, i.e., the zero-temperature carrier concentration $n = 2.07 \times 10^{20}$ cm $^{-3}$, and obtained residual resistivity $\rho_0 = 1.84$ m Ω cm from the Hamann's equation, we can evaluate the mean-free path of S-09, $l = 1.35$ nm using Drude model $l = \hbar(3\pi^2)^{1/3}/(e^2\rho_0 n^{2/3})$. This confirms that S-09 is a dirty-limit superconductor since $l/\xi(0) = 0.396$.

IV. CONCLUSION

In summary, the anisotropy in the upper critical field of $\text{Fe}_{1.14(1)}(\text{Te}_{0.91(2)}\text{S}_{0.09(2)})_z$ single crystals was studied in high and stable magnetic fields up to 35 T. We found that the zero-temperature upper critical field is much smaller than the predicted result of WHH theory without the spin-paramagnetic effect. The anisotropy of the upper critical field decreases with decreasing temperature, becoming nearly isotropic at low temperature. The spin-paramagnetic effect is

the dominant pair-breaking mechanism for both $H\parallel ab$ and $H\parallel c$ crystallographic axes. There is obvious spin-orbital scattering effect in this system. Our results show no abrupt change in the carrier density at the temperature of magnetic transition and considerable Kondo-type scattering effects on resistivity, MR, and Hall properties. All of these results indicate that the excess Fe in Fe(2) site act as Kondo-type impurities and play a key role in the exotic normal- and superconducting-state properties.

ACKNOWLEDGMENTS

We thank Vladimir Dobrosavljevic, Ruslan Prozorov, and

Weiguo Yin for useful discussions and T. P. Murphy for experiment support in NHMFL. This work was carried out at the Brookhaven National Laboratory, which is operated for the U.S. Department of Energy by Brookhaven Science Associates under Contract No. DE-Ac02-98CH10886. This work was in part supported by the U.S. Department of Energy, Office of Science, Office of Basic Energy Sciences as part of the Energy Frontier Research Center (EFRC), Center for Emergent Superconductivity (CES). A portion of this work was performed at the National High Magnetic Field Laboratory, which is supported by NSF Cooperative Agreement No. DMR-0084173, by the State of Florida, and by the U.S. Department of Energy.

*Present address: Ames Laboratory US DOE and Department of Physics and Astronomy, Iowa State University, Ames, IA 50011, USA.

- ¹Y. Kamihara, T. Watanabe, M. Hirano, and H. Hosono, *J. Am. Chem. Soc.* **130**, 3296 (2008).
- ²C. de la Cruz, Q. Huang, J. W. Lynn, J. Y. Li, W. Ratcliff II, J. L. Zarestky, H. A. Mook, G. F. Chen, J. L. Luo, N. L. Wang, and P. C. Dai, *Nature (London)* **453**, 899 (2008).
- ³I. I. Mazin, D. J. Singh, M. D. Johannes, and M. H. Du, *Phys. Rev. Lett.* **101**, 057003 (2008).
- ⁴K. Kuroki, S. Onari, R. Arita, H. Usui, Y. Tanaka, H. Kontani, and H. Aoki, *Phys. Rev. Lett.* **101**, 087004 (2008).
- ⁵W. Bao, Y. Qiu, Q. Huang, M. A. Green, P. Zajdel, M. R. Fitzsimmons, M. Zhernenkov, S. Chang, M. H. Fang, B. Qian, E. K. Vehstedt, J. H. Yang, H. M. Pham, L. Spinu, and Z. Q. Mao, *Phys. Rev. Lett.* **102**, 247001 (2009).
- ⁶M. D. Lumsden, A. D. Christianson, E. A. Goremychkin, S. E. Nagler, H. A. Mook, M. B. Stone, D. L. Abernathy, T. Guidi, G. J. MacDougall, C. de la Cruz, A. S. Sefat, M. A. McGuire, B. C. Sales, and D. Mandrus, *Nat. Phys.* **6**, 182 (2010).
- ⁷C.-C. Lee, W.-G. Yin, and W. Ku, *Phys. Rev. Lett.* **103**, 267001 (2009).
- ⁸F. C. Hsu, J. Y. Luo, K. W. Yeh, T. K. Chen, T. W. Huang, P. M. Wu, Y. C. Lee, Y. L. Huang, Y. Y. Chu, D. C. Yan, and M. K. Wu, *Proc. Natl. Acad. Sci. U.S.A.* **105**, 14262 (2008).
- ⁹K.-W. Yeh, T. W. Huang, Y. L. Huang, T. K. Chen, F. C. Hsu, P. M. Wu, Y. C. Lee, Y. Y. Chu, C. L. Chen, J. Y. Luo, D. C. Yan, and M. K. Wu, *EPL* **84**, 37002 (2008).
- ¹⁰Y. Mizuguchi, F. Tomioka, S. Tsuda, T. Yamaguchi, and Y. Takano, *Appl. Phys. Lett.* **94**, 012503 (2009).
- ¹¹A. Subedi, L. Zhang, D. J. Singh, and M. H. Du, *Phys. Rev. B* **78**, 134514 (2008).
- ¹²Y. Mizuguchi, F. Tomioka, S. Tsuda, T. Yamaguchi, and Y. Takano, *Appl. Phys. Lett.* **93**, 152505 (2008).
- ¹³L. J. Zhang, D. J. Singh, and M. H. Du, *Phys. Rev. B* **79**, 012506 (2009).
- ¹⁴R. W. Hu, E. S. Bozin, J. B. Warren, and C. Petrovic, *Phys. Rev. B* **80**, 214514 (2009).
- ¹⁵H. Q. Yuan, J. Singleton, F. F. Balakirev, S. A. Baily, G. F. Chen, J. L. Luo, and N. L. Wang, *Nature (London)* **457**, 565 (2009).
- ¹⁶J. Jaroszynski, F. Hunte, L. Balicas, Y.-J. Jo, I. Raičević, A. Gurevich, D. C. Larbalestier, F. F. Balakirev, L. Fang, P. Cheng, Y. Jia, and H. H. Wen, *Phys. Rev. B* **78**, 174523 (2008).
- ¹⁷F. Hunte, J. Jaroszynski, A. Gurevich, D. C. Larbalestier, R. Jin, A. S. Sefat, M. A. McGuire, B. C. Sales, D. K. Christen, and D. Mandrus, *Nature (London)* **453**, 903 (2008).
- ¹⁸H.-S. Lee, M. Bartkowiak, J.-H. Park, J.-Y. Lee, J.-Y. Kim, N.-H. Sung, B. K. Cho, C.-U. Jung, J. S. Kim, and H.-J. Lee, *Phys. Rev. B* **80**, 144512 (2009).
- ¹⁹S. A. Baily, Y. Kohama, H. Hiramatsu, B. Maiorov, F. F. Balakirev, M. Hirano, and H. Hosono, *Phys. Rev. Lett.* **102**, 117004 (2009).
- ²⁰M. Kano, Y. Kohama, D. Graf, F. Balakirev, A. S. Sefat, M. A. McGuire, B. C. Sales, D. Mandrus, and S. W. Tozer, *J. Phys. Soc. Jpn.* **78**, 084719 (2009).
- ²¹Z.-S. Wang, H.-Q. Luo, C. Ren, and H.-H. Wen, *Phys. Rev. B* **78**, 140501(R) (2008).
- ²²Z. Pribulova, T. Klein, J. Kacmarcik, C. Marcenat, M. Konczykowski, S. L. Bud'ko, M. Tillman, and P. C. Canfield, *Phys. Rev. B* **79**, 020508(R) (2009).
- ²³W. K. Kwok, S. Fleshler, U. Welp, V. M. Vinokur, J. Downey, G. W. Crabtree, and M. M. Miller, *Phys. Rev. Lett.* **69**, 3370 (1992).
- ²⁴H. Safar, P. L. Gammel, D. A. Huse, D. J. Bishop, J. P. Rice, and D. M. Ginsberg, *Phys. Rev. Lett.* **69**, 824 (1992).
- ²⁵H. C. Lei, R. W. Hu, E. S. Choi, J. B. Warren, and C. Petrovic, *Phys. Rev. B* **81**, 094518 (2010).
- ²⁶N. R. Werthamer, E. Helfand, and P. C. Hohenberg, *Phys. Rev.* **147**, 295 (1966).
- ²⁷G. Fuchs, S.-L. Drechsler, N. Kozlova, M. Bartkowiak, J. E. Hamann-Borrero, G. Behr, K. Nenkov, H.-H. Klauss, H. Maeter, A. Amato, H. Luetkens, A. Kwadrin, R. Khasanov, J. Freudenberger, A. Köhler, M. Knupfer, E. Arushanov, H. Rosner, B. Büchner, and L. Schultz, *New J. Phys.* **11**, 075007 (2009).
- ²⁸K. Maki, *Phys. Rev.* **148**, 362 (1966).
- ²⁹H. Kim, C. Martin, R. T. Gordon, M. A. Tanatar, J. Hu, B. Qian, Z. Q. Mao, R. W. Hu, C. Petrovic, N. Salovich, R. Giannetta, and R. Prozorov, *Phys. Rev. B* **81**, 180503(R) (2010).
- ³⁰P. Fulde and R. A. Ferrell, *Phys. Rev.* **135**, A550 (1964).
- ³¹A. I. Larkin and Y. N. Ovchinnikov, *Zh. Eksp. Teor. Fiz.* **47**, 1136 (1964) [*Sov. Phys. JETP* **20**, 762 (1965)].
- ³²A. Gurevich, *Phys. Rev. B* **67**, 184515 (2003).
- ³³M. H. Fang, J. H. Yang, F. F. Balakirev, Y. Kohama, J. Singleton, B. Qian, Z. Q. Mao, H. D. Wang, and H. Q. Yuan, *Phys. Rev. B*

- 81**, 020509(R) (2010).
- ³⁴G. Fuchs, S.-L. Drechsler, N. Kozlova, G. Behr, A. Köhler, J. Werner, K. Nenkov, C. Hess, R. Klingeler, J. E. Hamann-Borrero, A. Kondrat, M. Grobosch, A. Narduzzo, M. Knupfer, J. Freudenberger, B. Büchner, and L. Schultz, *Phys. Rev. Lett.* **101**, 237003 (2008).
- ³⁵T. P. Orlando, E. J. McNiff, Jr., S. Foner, and M. R. Beasley, *Phys. Rev. B* **19**, 4545 (1979).
- ³⁶M. Schossmann and J. P. Carbotte, *Phys. Rev. B* **39**, 4210 (1989).
- ³⁷B. C. Sales, A. S. Sefat, M. A. McGuire, R. Y. Jin, D. Mandrus, and Y. Mozharivskyj, *Phys. Rev. B* **79**, 094521 (2009).
- ³⁸T. J. Liu, X. Ke, B. Qian, J. Hu, D. Fobes, E. K. Vehstedt, H. Pham, J. H. Yang, M. H. Fang, L. Spinu, P. Schiffer, Y. Liu, and Z. Q. Mao, *Phys. Rev. B* **80**, 174509 (2009).
- ³⁹D. R. Hamann, *Phys. Rev.* **158**, 570 (1967).
- ⁴⁰P. Monod, *Phys. Rev. Lett.* **19**, 1113 (1967).
- ⁴¹C. Tarantini, M. Putti, A. Gurevich, Y. Shen, R. K. Singh, J. M. Rowell, N. Newman, D. C. Larbalestier, P. Cheng, Y. Jia, and H.-H. Wen, *Phys. Rev. Lett.* **104**, 087002 (2010).
- ⁴²H. Q. Luo, P. Cheng, Z. S. Wang, H. Yang, Y. Jia, L. Fang, C. Ren, L. Shan, and H. H. Wen, *Physica C* **469**, 477 (2009).
- ⁴³M.-T. Béal-Monod and R. A. Weiner, *Phys. Rev.* **170**, 552 (1968).
- ⁴⁴D. A. Whitney, R. M. Fleming, and R. V. Coleman, *Phys. Rev. B* **15**, 3405 (1977).
- ⁴⁵A. Fert, A. Friederich, and A. Hamzic, *J. Magn. Magn. Mater.* **24**, 231 (1981).
- ⁴⁶P. Cheng, H. Yang, Y. Jia, L. Fang, X. Y. Zhu, G. Mu, and H.-H. Wen, *Phys. Rev. B* **78**, 134508 (2008).
- ⁴⁷G. F. Chen, W. Z. Hu, J. L. Luo, and N. L. Wang, *Phys. Rev. Lett.* **102**, 227004 (2009).